

# 長期時域疲勞損傷模擬之數值收斂性探討於 套管式離岸風力機基礎結構

林宗岳\*<sup>1</sup> 吳凱洋\* 范秉天\*

黃心豪\*\* 簡志宇\*\*

\*財團法人中國驗船中心 研究處研發組  
\*\*國立台灣大學 工程科學及海洋工程學系

關鍵詞：離岸風力機，套管式基礎結構，疲勞壽命，時域分析

## 摘要

本研究以時域法分析套管式離岸風力機基礎結構的疲勞壽命。此離岸風力機容量為 3.6 MW，設定場址位於台灣海峽。海上環境量測及統計資料來源取自三年期的初期場址調查，得到風況及海況的機率散佈表和聯合機率表，以此決定需要計算的環境狀況。環境負荷使用 BEM 準穩態時域計算風負荷和 HydroCrest 軟體計算圓管構件之波浪負荷。結構分析由樑元件有限元素分析接點公稱應力，搭配應力集中係數、兩流計數法和 S-N 曲線，得到接點疲勞壽命。以時域法模擬疲勞問題最大困難在於計算耗時長且需模擬長達 20 年的歷程；前者於本研究中改良 HydroCrest 和公稱應力演算法，大幅縮短計算時間；後者則需探討模擬時間長度和時間步進對疲勞損傷之統計特性的影響，以決定最短模擬時間和最大時間步進，使之在最少計算步之內達到收斂。在 16 個不同短期環境條件時間和時間步進設定中，30 分鐘和 1.0 秒之組合，共計 1500 萬計算步方能得到收斂的 20 年疲勞累積破壞值；疲勞熱點發生於下層腳管與連桿的 K 接點，疲勞損傷值為 0.489。此結果仍需要以長時間的實際量測資料確認正確性。

## Introduction

Taiwan has recently started to evaluate the potential for offshore wind energy production off its west coast, which was selected by 4C Offshore Limited as one of the world's best wind locations [1], having considerable development potential due to high wind energy, stable wind speed, and shallow water depth.

The authors [2, 3] previously showed that typhoon conditions are crucial design problems for the ultimate strength of the unit. However, fatigue strength can be just as significant, especially at the tubular joint connections of the jacket support structure that are subjected to numerous load cycles during the 20 years of design life. To this end, the authors [4] recently conducted time-domain simulations to reproduce the long-term evolution of the wind and wave loads on the unit and to evaluate the corresponding structural response. This was done by collating joint probability tables to produce a covariance matrix for the considered environmental load parameters, namely wave height, wave period, and wind speed, and then stochastically gener-

ate the desired 20 years of weather states through Cholesky decomposition of said covariance matrix.

While this recent study was highly beneficial in terms of validating the adopted Finite Element-derived Closed Form (CF) approach, not to mention demonstrating the low damage inflicted upon the jacket foundation's X-joints, a lack of sufficiently detailed environmental data led the authors to implement the present study, which seeks to provide a more accurate fatigue life assessment based on the probabilities of occurrence of each combination of environmental parameters, taken directly from a set of decomposed joint probability tables, while further reducing computation times.

Due to the long computation times of time-domain simulations, this study adopted the same wave load generation models and CF structural response approaches that were previously shown to be a good trade-off between time-efficiency and simulation accuracy, as well as a more realistic wind load generation model. The calculations were conducted according to DNVGL Guideline [5], in compliance with the IEC's 61400-1 International Standard [6].

---

<sup>1</sup> 林宗岳 (tylin@crlclass.org)

The long-term environmental conditions are described in the second section of this paper, and the short-term conditions, based on IEC and DNV guidelines, and the numerical models employed to calculate the wind and hydrodynamic loads are described in the third and fourth parts. The fifth part of the present paper presents the hot spot stress evaluation approach that combined FE-derived Closed-Form expressions of the nominal stresses at the tubular joints and stress concentration factors. Finally, the fatigue damage was assessed using the Rainflow Cycle Counting scheme. The fatigue life assessment results and suggestions for future improvements are discussed in the Conclusions.

### Long-term Statistical Representation of Environment

The long-term statistical environment was based on a preliminary site survey gathered over three years. In this survey, six scatter diagrams, showing the number of one-hour observations of each significant wave height and peak wave period ( $H_s$ - $T_p$ ), were presented for a range of hub height wind speeds  $U_{hub}$ . Joint probability tables for wind speed, wind direction, wave height, and wave period were analyzed, and, based on a strong correlation between wind speed and wave height, i.e.  $\text{corr}(U_{hub}, H_s) = 0.72$ , and high similitude between the normalized component probability distributions for wind direction  $\theta_{wnd}$ , which suggested that  $U_{hub}$ - $\theta_{wnd}$  joint probabilities could be uniformly applied to the other parameters, each of the six  $H_s$ - $T_p$ - $U_{hub}$  diagrams were further decomposed into twelve tables, one per wind direction, such that the probability of occurrence of each combination of said environmental parameters could be easily referenced from 72  $H_s$ - $T_p$ - $U_{hub}$ - $\theta_{wnd}$  joint probability tables, with a total of 120  $H_s$ - $T_p$  probabilities per table  $\times$  72 tables = 8640 combinations.

In this way, the contribution of each short-term condition to the total fatigue life was weighted by its frequency of occurrence, such that the fatigue damage was mostly driven by frequently occurring mild wind and wave conditions, as opposed to extreme conditions, such as typhoons, that occur more seldom, and would represent only a small part of the total fatigue life of the structure.

### Short-term Time Domain Wave Loads

For each sea state, the selected JONSWAP sea spectrum [7] and directional spreading function were applied to obtain an irregular, time-varying flow field, for which the consequent wave loads were determined by the Morison equation, as expressed in Eq. (1), executed via the in-house **HydroCrest** code. The determination of coefficients follows DNVGL Guideline [5],

where the slamming term  $F_s$  is neglected in normal wave conditions.

Based on the superposition solution of potential flow theory, an irregular sea surface can be decomposed into an infinite number of regular component waves, which are formulated by amplitude, direction, frequency, and phase. For a given power spectrum, i.e. directional JONSWAP, Eq. (2), the amplitude is calculated by Eq. (3). The JONSWAP formula is expressed by Eq. (4), and the directional spreading function is the cosine-power equation, as Eq. (5). A GPU accelerator was utilized [9] to speed up the wave load simulation for parallel processing thousands of component waves and element nodes and then sum reduction of each line load to an overall overturning moment to comply with the close-form formulation of FEA. Figure 1 shows the nodal forces and total force in **HydroCrest**. Figures 2 plot the time series of OTM magnitude of the two demonstrated spectrums at  $H_s = 1.4\text{m}$  and  $4.0\text{m}$ .

$$F_M = \rho_{sw} \cdot C_M \cdot A \cdot \dot{v} + \frac{1}{2} \rho_{sw} \cdot C_D \cdot D \cdot v \cdot |v| + F_s \quad (1)$$

$$E(\omega, \theta) = S_j(\omega) D(\omega, \theta) \quad (2)$$

$$a(\omega_n, \theta_n) = \sqrt{2 \int_{\Delta\omega_n} \int_{\Delta\theta_n} E(\omega, \theta) d\theta d\omega} \quad (3)$$

$$\approx \sqrt{2 S_j(\omega_n) D(\omega_n, \theta_n) \Delta\theta \Delta\omega} \quad (3)$$

$$S_j(\omega) = \frac{\alpha g^2}{\omega^5} \exp\left(-1.25 \left(\frac{\omega_p}{\omega}\right)^4\right) \gamma \exp\left(-\frac{(\omega - \omega_p)^2}{2\sigma^2 \omega_p^2}\right) \quad (4)$$

$$D(\omega, \theta) = N(s(\omega)) \cos^{2s(\omega)}\left(\frac{\theta_w - \theta}{2}\right) \quad (5)$$

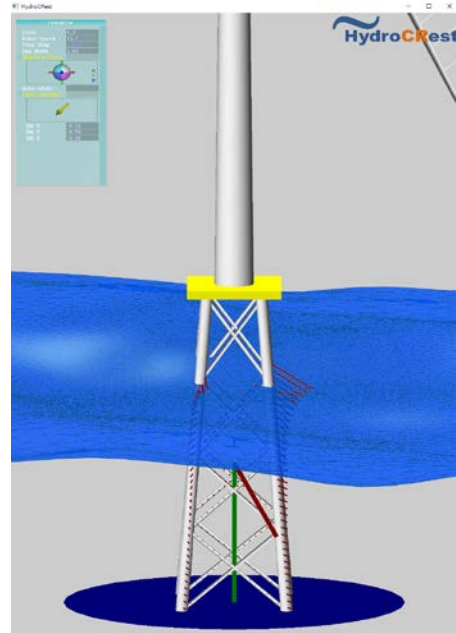


Figure 1. Nodal load distribution on members (thin lines) and total load (thick lines) in irregular sea

## Short-term Time Domain Wind Loads

On the short-term wind model, the concept of wind turbulence is explained in DNV [5] as “the natural variability of the wind speed about the mean wind speed  $U_{10}$  in a 10-minute period” for which “the short-term probability distribution for the instantaneous wind speed  $U$  can be assumed to be a normal distribution” with standard deviation  $\sigma_U$ . In the present study, the short term wind states were modeled on the IEC 61400-1 Normal Turbulence Model (NTM) [6], with a reference turbulence intensity of  $I_{ref} = 0.16$ , as per the requirement of the Taiwanese Ministry of Economic Affairs [10] that the pilot wind turbine to be installed in the Taiwan Strait Offshore Wind Farm must be IEC 61400-1 Class I<sub>A</sub> compliant. Following the NTM, the standard deviation  $\sigma_U$  of the wind speed for a given  $U_{10}$  is calculated by Eq. (6):

$$\sigma_U = I_{ref}(0.75 U_{10} + 3.8) \quad (6)$$

In order to generate a more realistic short-term wind state, the wind speed fluctuations were calibrated against real on-site data by applying a non-linear least squares regression analysis to the fast Fourier transforms (FFT) of the wind speed data over consecutive 10-minute periods, and then reconstructing the signals (Fig. 3 – top). The wind fluctuations were then further randomized by randomizing the phase shifts of the component harmonics (Fig. 3 – bottom). The regression curve amplitudes were then scaled so as to produce a final signal which conforms to the IEC NTM.

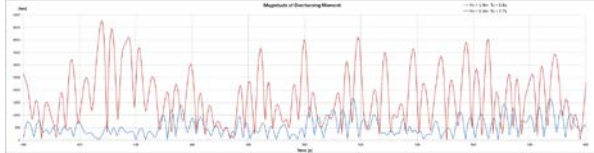


Figure 2. Time-history of magnitudes of overturning moments in two sea states

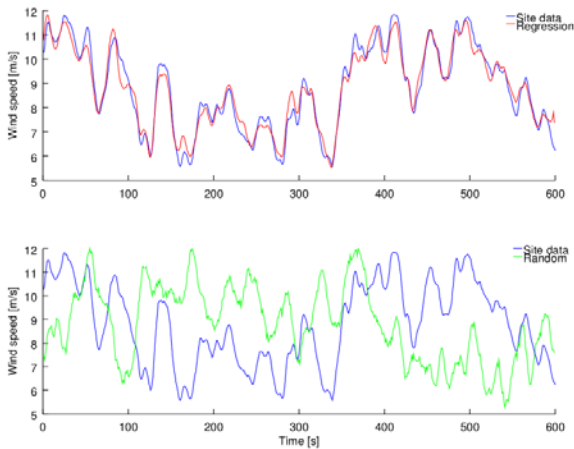


Figure 3. Reconstructed FFTs of real wind data

Due to the large number of transient wind load calculations to be made over the simulated life time, an unsteady blade element momentum method (UBEM) was adopted to calculate the aerodynamic loads on the wind turbine. Due to its maturity, the BEM is widely employed for the design and analysis of wind turbines [11]. The blade element theory discretises the rotor into a number of 2D airfoil sections, such that the axial and tangential loads on each 2D section may be calculated from the respective airfoil’s lift and drag characteristics for the respective local relative flow velocity and angle. These local loads are then integrated along the length of the rotor blades and multiplied by the number of blades, as per Eq. (7), to determine the total thrust and rotor torque:

$$\begin{aligned} dF_N &= n_B \frac{1}{2} \rho U_{rel}^2 \int_0^R (C_{l1} \cos \varphi + C_{d1} \cos \varphi) c dr \\ dQ &= n_B \frac{1}{2} \rho U_{rel}^2 \int_0^R (C_{l1} \sin \varphi + C_{d1} \cos \varphi) c r dr \end{aligned} \quad (7)$$

The BEM model was validated against the power curve provided by the 3.6 MW wind turbine manufacturer [12] for the full range of normal operating conditions, taking into consideration cut-in, cut-out, and supra-nominal (pitch control) wind velocities, and was found to correlate very well with the official data.

To account for stochastic loading, due to fluctuating wind speeds, and deterministic cyclic loading, due to rotor-tower interaction, wind shear profile due to friction with the ocean surface, and tilt angle effects, the wind turbine rotor plane was discretized onto a radial grid, such that the Cartesian coordinates of the blade elements (taking into consideration tilt, coning angle, and rotor overhang (Fig. 4)) are known throughout the rotor plane, thereby allowing for easy computation of relative wind components in terms of each blade element’s local coordinate system. In this way, the wind load time step is easily set via the angular component of the radial grid.

The effects of the wind turbine tower on the upstream flowfield were modelled by assuming potential flow around a circular cylinder [13] (Fig. 5), such that the radial and angular components of the flow velocity at a considered point are given by Eq. (8):

$$\begin{aligned} U_r &= U_\infty \left(1 - \frac{R^2}{r^2}\right) \cos \theta \\ U_\theta &= -U_\infty \left(1 + \frac{R^2}{r^2}\right) \sin \theta \end{aligned} \quad (8)$$

A wind shear profile was included, such that the wind velocity at height  $z$  for a specified hub height velocity  $U(H)$  is given by Eq. (9):

$$U(z) = U(H) \left(\frac{z}{H}\right)^\alpha \quad (9)$$

where the power law exponent for offshore locations is taken as  $\alpha = 0.14$ , in accordance with DNV [5].

## Closed-form Evaluation of Hot Spot Stress

Using beam elements, a structural finite element model of the unit was built, which included the tower, the mass of the rotor nacelle assembly, the jacket, and the four piles, for which the interaction with the soil was reproduced using nonlinear elastic spring connectors. The wind thrust at the nacelle and hydrodynamic line loads on the jacket were produced by **HydroCrest**. Figure 6 shows the finite element model of the offshore wind turbine. The computation time required to conduct the static Finite Element Analyses was approximately 0.5 s per time step, which would require several weeks of computations for the millions of wind and wave induced load cycles to simulate during a 20-year design life. A faster approach was thus adopted to conduct rapid fatigue life assessments that consisted in deriving from FEA results the Closed-Form (CF) expressions of the nominal stress at the tubular joints connection in the jacket structure as a function of four global load parameters (Fig. 6):

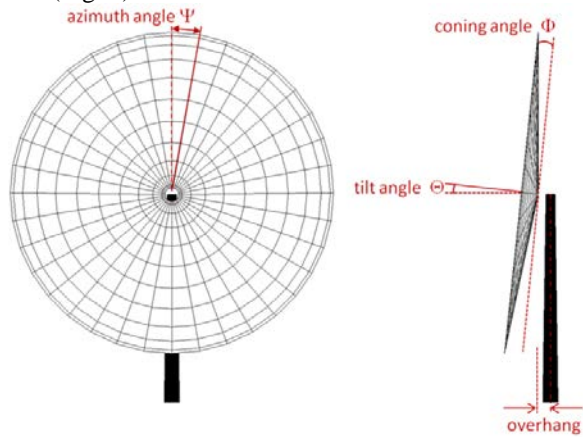


Figure 4. Discretised rotor plane

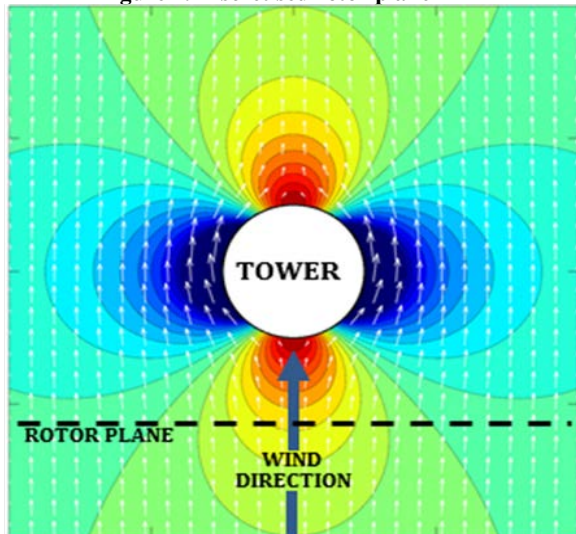


Figure 5. Potential flow tower model

- the amplitude and direction of the hydrodynamic load (i.e. wave and current on jacket) induced overturning moment at the mudline ( $OTM_{Hydro}$  and  $\beta_{Hydro}$ ), and
- the amplitude and direction of the wind load (i.e. tower and blades) induced overturning moment at the mudline ( $OTM_{Wind}$  and  $\beta_{Wind}$ ).

The structural stress assessment at the joints for more than 8000 wind and wave load combinations were conducted through static FEAs that corresponded to various combinations in amplitude and directions of the 4 global load parameters entailed in the Closed-Form expression. A unique regression expression was then fitted for each FE-nodal stress at the joints' connections through a set of constant parameters ( $C_1$  to  $C_8$ ) as provided in Eq. (10).

$$\sigma_{nom} = (C_1 \cdot OTM_{Wind} + C_2) \cdot \cos(\beta_{Wind} + C_3) + C_4 \cdot \cos(\beta_{Hydro} + C_5) + (C_6 \cdot OTM_{Hydro}^2 + C_7 \cdot OTM_{Hydro} + C_8) \quad (10)$$

The nominal stresses at 545 nodes in the global FE model produced by the Closed-Form expressions and those extracted from the global FEA for 8321 FE-load combinations and two different water depths. The Closed-Form expressions were determined using the FE-results corresponding to the average high-tide water depth FE-load cases. The same Closed-Form expressions were then employed to reproduce the nominal stresses computed for the low-tide FE-load cases, and it appeared that the accuracy was still satisfactory despite a hydrodynamic line load distribution obtained for a water depth 3.5 m shallower. The Closed-Form nominal stress expressions approach enabled a significant reduction of the computation time to approximately 0.722 ms per time step. Finally, the hot spot stresses at 8 spots around the circumference of the considered connection were obtained by including the stress concentration factors according to DNVGL [14].

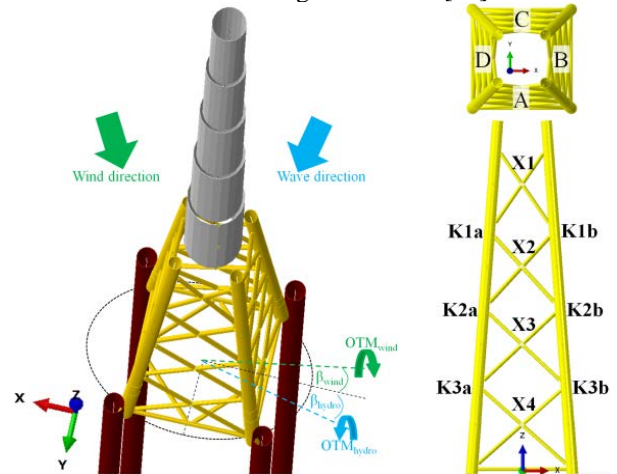


Figure 6. Offshore wind turbine finite element model and CF expressions for load parameters at the mudline.

## Fatigue Assessment

This study examined the fatigue life of 6 K-joints on each face of the jacket (Fig. 6). Those joints' locations were deemed sufficiently remote from the tower's flange and pile sleeve connections' influence that were approximately represented in the FE model through rigid kinematic couplings. Therefore, at those joints, the nominal stress approach, as described in the previous section, would provide sufficient accuracy for the fatigue analysis. The hot spot stress was then calculated at 8 spots around the circumference of the intersection on the brace and the chord side according to DNVGL [14] formulations.

For the most contributing wind speed of 17.5 m/s, a sensitivity study was conducted to evaluate the accuracy of the fatigue damage prediction for various short-term environment condition settings in terms of:

- duration: 10 min, 20 min, 30 min and 60 min,
- time-step interval: 0.25 s, 0.75 s, 1.0 s and 1.5 s.

The reference computation entailed a 60-min load duration, which is consistent with the long term wave and wind observations in the scatter diagrams, and a 0.25 s time-step that enabled our wind/wave load models to capture very short variations of load such as the tower effects and the smallest component waves. The results produced for this setting will be employed as reference basis for the comparison with other settings.

The stress distribution was then obtained by the Rainflow Counting stress Cycles method, and the fatigue damage was produced for the 'T' class S-N curve provided by DNVGL [14]. Since the short-term environmental conditions were defined for different duration  $t$ , the damage was scaled up to the 20-year design life as expressed in Eq.(11) to be comparable.

$$D_{20yrs} = \frac{20 * 365.25 * 24 * 60}{t} D_{t-min} \quad (11)$$

**Table 1. Fatigue damage accuracy**

t [min]	Δt [s]	N <sub>time-step</sub>	D <sub>t-min</sub>	D <sub>20yrs</sub>	Accuracy
10	0.25	2400	1.083E-06	1.14	141%
10	0.75	800	1.054E-06	1.11	138%
10	1	600	1.049E-06	1.10	137%
10	1.5	400	1.003E-06	1.06	131%
20	0.25	4800	1.717E-06	0.90	112%
20	0.75	1600	1.658E-06	0.87	108%
20	1	1200	1.684E-06	0.89	110%
20	1.5	800	1.544E-06	0.81	101%
30	0.25	7200	2.055E-06	0.72	90%
30	0.75	2400	1.995E-06	0.70	87%
<b>30</b>	<b>1</b>	<b>1800</b>	<b>2.012E-06</b>	<b>0.706</b>	<b>88%</b>
30	1.5	1200	1.841E-06	0.65	80%
60	0.25	14400	4.592E-06	0.81	100%
60	0.75	4800	4.449E-06	0.78	97%
60	1	3600	4.459E-06	0.78	97%
60	1.5	2400	4.314E-06	0.76	94%

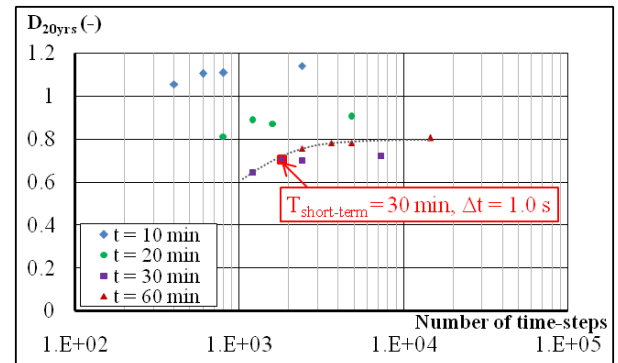
Figure 7 shows the damage predictions and their related numbers of time steps, which represent time of computation. It can be observed that the damages obtained for 10-min and 20-min durations overestimated the damage obtained by the reference computation, while for the 30-min duration the results were converging. Additionally, the time-step intervals 0.75 s to 1.0 s resulted in good accuracy of damage prediction compared to the reference 0.25 s setting, whereas for Δt = 1.5 s the damage predictions were significantly underestimated.

Figure 8 shows the stress range distribution obtained by Rainflow stress cycle counting method for various load durations. It appeared that the stress range distribution produced for the 10-min load duration overestimated that obtained for the 60-min duration, whereas for the 20-min and especially the 30-min durations, the distributions came very close to the reference calculation. This is consistent with the damage results observations made in Figure 7.

Table 1 lists the damage results and shows the accuracy of the damage in terms of ratio of the damage prediction for given load settings to the reference damage produced for 60 min short-term condition duration and 0.25 s time step interval. An optimal setting of 30 min duration for 1.0 s time-step interval was found to be a good tradeoff between accuracy (88%) and fast computation (1800 time-steps) and will be employed for the fatigue assessment.

**Table 2. Fatigue damage results**

Tubular joint	Fatigue damage for 20 years design life (-)			
	Face A	Face B	Face C	Face D
K1a	0.044	0.242	0.044	0.244
K1b	0.353	0.079	0.352	0.080
K2a	0.011	0.168	0.011	0.170
K2b	0.162	0.013	0.159	0.013
K3a	0.076	<b>0.304</b>	0.076	<b>0.304</b>
K3b	<b>0.489</b>	0.024	<b>0.484</b>	0.023



**Figure 7. Damage predictions vs. time of computation for various load settings.**

For each of the 8640 short-term conditions the fatigue damage was evaluated as previously described. The total fatigue damage was then produced as the sum of all the damage weighted by its corresponding long-term statistical frequency. Table 2 presents the fatigue damage of the tubular joints in the jacket. It can be observed that the most critical joints were the K3 'a' and 'b' that were located low in the jacket and thus underwent high levels of stresses, especially from the legs. Additionally, the short-term condition that contributed the most to the fatigue was that with a 22.5 m/s wind speed, which is just before the cut-out speed of 25 m/s, a significant wave height of 2.25 m, and zero-crossing period of 7.5 s.

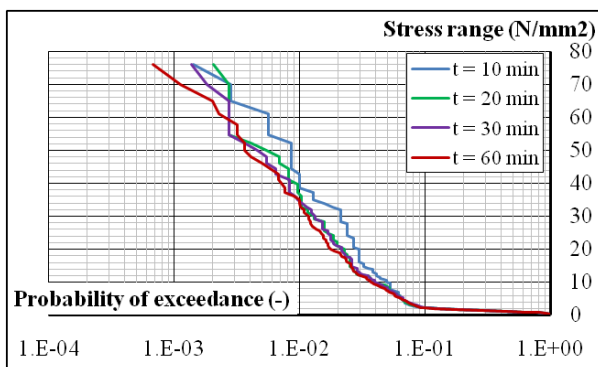


Figure 8. Stress range distribution for various short-term durations and  $\Delta t = 0.25$  s.

## Conclusions

This study presented a fatigue life evaluation methodology for fixed-type offshore wind turbine foundations using time-domain simulations and the Rainflow Cycle Counting method. A long-term statistical environment, based on a preliminary site survey comprising three years' worth of one-hour observations served as the basis for a convergence study for an accurate fatigue life evaluation. Short-term conditions based on IEC and DNV guidelines were generated for a number of load durations and time steps, and an optimal load setting of 60-min short-term environmental conditions with 1.0 s time-steps was then selected based on a sensitivity study on the fatigue damage prediction. After analysis, an insufficient fatigue strength was identified which would require further calculations involving more extensive long-term data measurements in order to confirm those critical results.. Longer simulations are thus required in order to determine an optimal life time of simulation that, in the future, could be employed to conduct time-efficient fatigue assessment entailing global finite element analyses.

## Reference

- [1] "Offshore Wind Farms Database," <http://www.4coffshore.com>, 2015
- [2] T.Y. Lin, Y. Quéméner, "Extreme Typhoon Loads Effect on the Structural Response of Offshore Meteorological Mast and Wind Turbine", Proceedings of the ASME 2016 35th International Conference on Ocean, Offshore and Arctic Engineering, OMAE2016, 19-24 Jun., 2016, Busan, Korea.
- [3] B. Nelson, T.Y. Lin, Y. Quéméner, H.H. Huang, C.Y. Chien, "Extreme Typhoon Loads Effect on the Structural Response of an Offshore Wind Turbine", Proceedings of 7th PAAMES and AMEC2016, 13-14 Oct., 2016, Hong Kong.
- [4] T.Y. Lin, Y. Quéméner, B. Nelson, H.H. Huang, C.Y. Chien, "Fatigue Life Evaluation using Time-domain Simulation for Bottom-fixed Jacket Foundation of Offshore Wind Turbine", Proceedings of 2016 Taiwan Wind Energy Conference, 1 Dec., 2016, Keelung, Taiwan
- [5] DNVGL (2014), Design of Offshore Wind Turbine Structures, DNVGL-OS-J101.
- [6] IEC, Wind turbines – Part 1: Design requirements, IEC International Standard 61400-1, 2005.
- [7] Hasselmann, K., Barnett, T.P. et al., "Measurements of wind-wave growth and swell decay during the Joint North Sea Wave Project (JONSWAP)" TU Delft, 1973.
- [8] Jocelyn Frechot "REALISTIC SIMULATION OF OCEAN SURFACE USING WAVE SPECTRA"
- [9] "Nvidia CUDA C Programming Guide", NVIDIA, 2014
- [10] Ministry of Economic Affairs of Taiwan (R.O.C.), "風力發電離岸系統示範獎勵辦法 (Regulations for Demonstration and Rewards of Offshore Wind Power System)", Taiwan, 2012.
- [11] L. Kristensen, G. Jensen, A. Hansen, and P. Kirkegaard, "Field Calibration of Cup Anemometers", Risø-R-1218(EN), Risø National Laboratory, Roskilde, Denmark, 2001
- [12] Siemens brochure, "Thoroughly tested, utterly reliable: Siemens Wind Turbine SWT-3.6-120", Germany, 2011.
- [13] M. Hansen, *Aerodynamics of Wind Turbines*, 2nd Ed., Earthscan, London, UK, 2007.
- [14] DNVGL (2016), Fatigue design of offshore steel structures, DNVGL-RP-C203
- [15] L. Johansson, The importance of data availability: Effects of missing or erroneous data, EWEA 2013, Vienna, Austria

# Numerical Convergence Study of Long-term Time-domain Fatigue Damage Simulation for Jacket Foundation of Offshore Wind Turbine

*Tsung-Yueh Lin\*<sup>1</sup> Yann Quéméner\* Bryan Nelson\*  
Hsin-Haou Huang\*\* Chi-Yu Chien\*\**

\*R/D Section, Research Department, CR Classification Society, Taiwan

\*\*Department of Engineering Science and Ocean Engineering, National Taiwan University, Taipei, Taiwan

*Keywords: Offshore Wind Turbine, Jacket Foundation, Fatigue Life, Time-domain Simulation*

## ABSTRACT

This study evaluated the fatigue life of the jacket support structure of a 3.6 MW wind turbine operating in an offshore wind farm by time-domain simulations. The long term statistical environment was based on the wind-wave scatter diagrams and joint probability tables of a preliminary site survey that define total load cases. The wave loads were determined by the in-house **HydroCRest** code, and the wind loads by an unsteady BEM method. The Finite Element model of the jacket foundation was built using Beam elements. Nominal stresses at the tubular joints were extracted and stress concentration factors were applied to obtain the hot spot stress. The fatigue damage was then assessed for an adequate S-N curves through the Rainflow Cycle Counting scheme. Computational expense and simulation times for such time domain analyses are typically very high; we therefore improved the algorithm of **HydroCRest** and combined FE-derived Closed-Form expressions of the nominal stress to reduce the computational time, and conducted a convergence study to minimize the number of time steps for the accumulated fatigue damage prediction over 20 years. An optimal load setting of 30-min short-term environmental conditions with 1.0 s time-steps (interval) was employed to assess the fatigue life of the jacket. As a result, a critical fatigue damage value of 0.489 was predicted at the bottom leg-brace K-joints. Further calculations involving more extensive long-term data measurements in order to confirm those results.